MCB
Journals.ASM.org

Conserved Molecular Interactions within the HBO1 Acetyltransferase Complexes Regulate Cell Proliferation

Nikita Avvakumov,[a] Marie-Eve Lalonde,[a] Nehmé Saksouk,[a] Eric Paquet,[a] Karen C. Glass,[b]* Anne-Julie Landry,[a] Yannick Doyon,[a] Christelle Cayrou,[a] Geneviève A. Robitaille,[a] Darren E. Richard,[a] Xiang-Jiao Yang,[c] Tatiana G. Kutateladze,[b] and Jacques Côté[a]

Laval University Cancer Research Center, Hôtel-Dieu de Québec (CHUQ), Quebec City, Quebec, Canada[a]; Department of Pharmacology, University of Colorado at Denver, Aurora, Colorado, USA[b]; and Goodman Cancer Centre, McGill University and Department of Medicine, McGill University Health Centre, Montreal, Quebec, Canada[c]

Acetyltransferase complexes of the MYST family with distinct substrate specificities and functions maintain a conserved association with different ING tumor suppressor proteins. ING complexes containing the HBO1 acetylase are a major source of histone H3 and H4 acetylation *in vivo* and play critical roles in gene regulation and DNA replication. Here, our molecular dissection of HBO1/ING complexes unravels the protein domains required for their assembly and function. Multiple PHD finger domains present in different subunits bind the histone H3 N-terminal tail with a distinct specificity toward lysine 4 methylation status. We show that natively regulated association of the ING4/5 PHD domain with HBO1-JADE determines the growth inhibitory function of the complex, linked to its tumor suppressor activity. Functional genomic analyses indicate that the p53 pathway is a main target of the complex, at least in part through direct transcription regulation at the initiation site of p21/CDKN1A. These results demonstrate the importance of ING association with MYST acetyltransferases in controlling cell proliferation, a regulated link that accounts for the reported tumor suppressor activities of these complexes.

Members of the ING (*in*hibitor of *g*rowth) family of growth regulators are present in all eukaryotes, with the five human proteins (ING1 to ING5) and the three from *Saccharomyces cerevisiae* (Yng1, Yng2, and Pho23) being the most studied. Their homology is highest at the carboxyl termini within a *p*lant *h*omeo*d*omain (PHD) finger—a motif common to many chromatin regulatory proteins (8, 54). Expression analyses of several tumor types show that ING genes are either mutated or downregulated in many forms of cancer (43, 73), and a number of studies have implicated the ING proteins in the regulation of the cell cycle and proliferation, cellular aging and senescence, hormone signaling pathways, brain tumor growth, and angiogenesis (reviewed in reference 51). These functions stem from direct mechanistic roles in chromatin modification and remodeling, gene-specific transcription regulation, and DNA repair, recombination, and replication (2, 54, 61).

The multisubunit protein complexes containing ING family members have been purified and characterized from yeast and human cells (reviewed in references 2 and 54). The human INGs can be divided into three groups—ING1/2, ING3, and ING4/5—based on their association with three distinct types of protein complexes (8). Each of these complexes regulates chromatin modification and structure via histone acetylation and deacetylation. The ING complexes that carry out histone acetylation contain members of the MYST family of histone acetyltransferases (HATs) as their catalytic subunits (Fig. 1A). Human MYST HATs include Tip60 (KAT5), HBO1 (KAT7), MOZ (KAT6A), MORF (KAT6B), and MOF (KAT8). These enzymes are also known to play crucial roles in transcription activation and in DNA repair, recombination, and replication and are implicated in development and many human diseases, most notably cancer (2, 14, 69, 72).

Together with other histone-modifying enzymes, MYST acetyltransferases are key players in regulating local and global chromatin dynamics. The protruding tails of nucleosomal histones are substrates for a large number of posttranslational modifications, such as acetylation, methylation, phosphorylation, ubiquitination, and sumoylation (22). Different combinations of these modifications can regulate each other and establish an epigenetic signature that can be read by specific protein domains present in nuclear effector proteins, such as chromodomains, bromodomains, Tudor domains, MBT domains, and PHD fingers (27, 64).

Interestingly, many reports have identified the PHD finger as an important effector domain that selectively binds to the trimethylated lysine 4 residue of histone H3 (H3K4me3), a mark preferentially located at promoters and immediately downstream of transcription start sites (TSS) (30, 32, 34, 41, 45, 52, 56, 67, 71). Significantly, all PHD domains of the ING family members were shown to bind preferentially to this histone modification with strong dissociation constants (K_ds of <10 μM) (41, 56). Notably, yeast Yng1 PHD finger binds H3K4me and allows the associated NuA3 HAT complex to bind and acetylate chromatin (33, 63). Moreover, in response to DNA damage, the PHD domain of human ING2 binds with high affinity to H3K4me3, which stabilizes the association of the mSin3-HDAC1/2 (HDAC stands for histone deacetylase) complex at the promoters of proproliferation genes and represses their transcription (56). Similarly, HBO1-ING4/5 complexes were shown to functionally interact with H3K4me3

Received 19 October 2011 **Returned for modification** 15 November 2011
Accepted 27 November 2011

Published ahead of print 5 December 2011

Address correspondence to Jacques Côté, jacques.cote@crhdq.ulaval.ca.

* Present address: Department of Pharmaceutical Sciences, Albany College of Pharmacy and Health Sciences, Colchester, Vermont, USA.

N. Avvakumov and M.-E. Lalonde contributed equally to this article.

Supplemental material for this article may be found at http://mcb.asm.org/.

doi:10.1128/MCB.06455-11

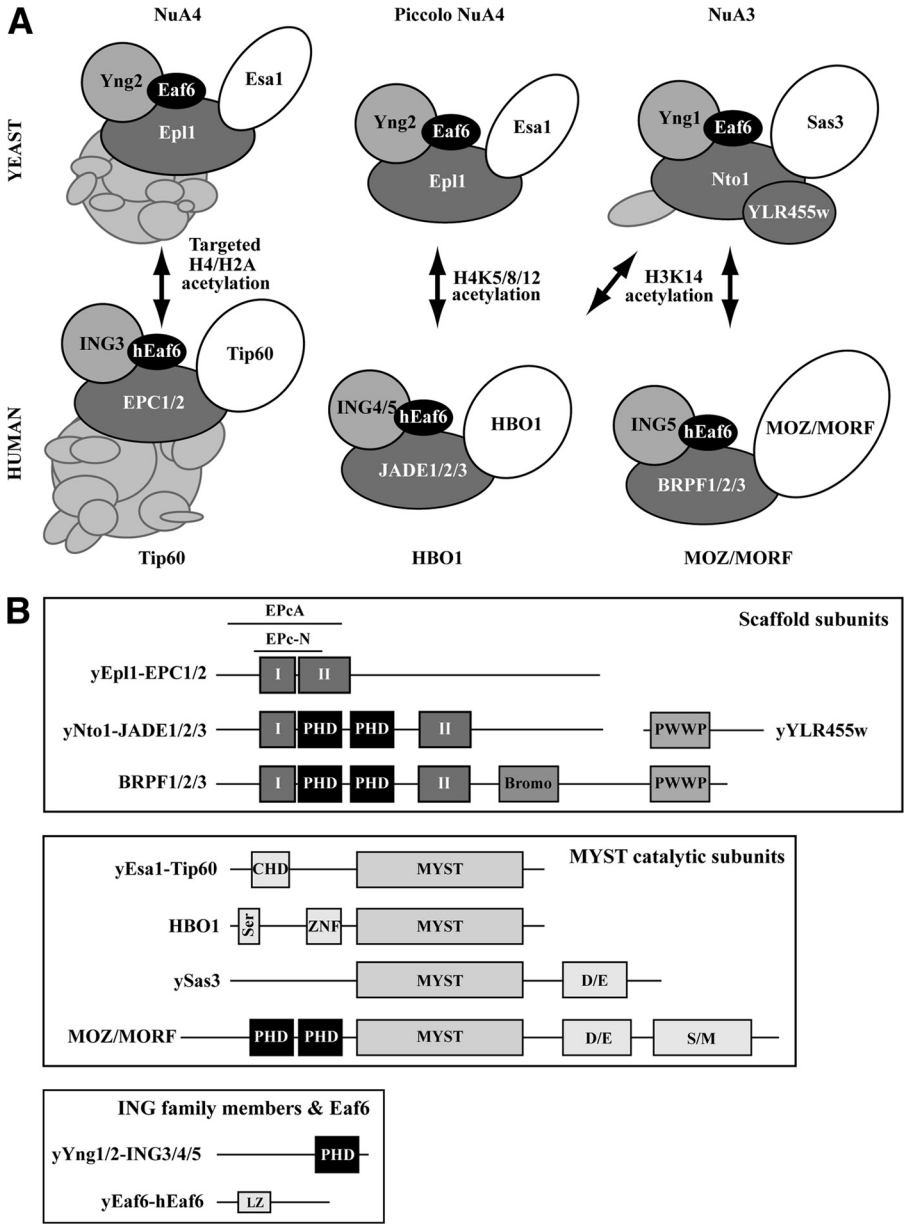

FIG 1 Common features of the MYST-ING histone acetyltransferase complexes. (A) Structural and functional conservation of MYST-ING HAT complexes from yeast to human. (B) Homologous core subunits of all MYST-ING complexes and their associated protein domains. Domains not mentioned in the text: Bromo, bromodomain; CHD, chromodomain; Ser, serine-rich; ZNF, zinc finger; D/E, acidic; S/M, serine/methionine-rich; LZ, leucine zipper. The previously identified domains EPcA in EPC, E(Pc) and Epl1, Epc-N and I/II in Epl1, Nto1, EPC, JADE, and BRPF are also identified (8, 42, 62).

chromatin, acetylate surrounding histone tails, and stimulate local transcription (18, 53). Thus, these findings suggest that the MYST-ING protein complexes contribute to epigenetic regulation of nuclear functions through cross talk between histone methylation and acetylation.

Interestingly, two new classes of chromatin-interacting PHD fingers have been identified more recently. In striking contrast to the original, PHDs of the second class bind the histone H3 N-terminal domain only when the lysine 4 residue is not methylated (20, 25). The third class was shown to be important for binding to chromatin by the yeast RPD3S deacetylase complex irrespective of histone marks (28). We recently demonstrated that both new types of PHD fingers are present in the JADE subunit of the HBO1-ING complexes and that they are essential for binding to chromatin *in vivo* (53). Strikingly, these features mean that a single HBO1 complex harbors PHD fingers of all three classes, with different specificities toward histone H3 lysine 4 methylation.

We have also previously characterized the human MYST-ING HAT complexes and highlighted their different specificities and functions (8). All MYST-ING complexes from yeast to humans appear to contain a core of 4 subunits that share significant homologies (Fig. 1). In addition, these subunits carry several domains with potential for reading different chromatin marks (Fig.

1B). Here we report the molecular dissection of MYST-ING HAT complexes *in vitro* and *in vivo*. We focused on the human ING4/5 tetrameric complexes that contain the HBO1 HAT and JADE1/2/3 paralogues (Fig. 1A), as they constitute one of the major sources of histone H4 and H3 acetylation *in vivo* (8, 23, 68). Notably, we identified two short domains conserved in all MYST-ING complexes that act as a scaffold for complex assembly. Interestingly, alternative mRNA splicing within these domains produces two distinct isoforms of JADE1, whose incorporation into the complex specifically regulates the association of ING4/5 with HBO1. An array of techniques, including cell growth assays, gene expression analysis, and chromatin immunoprecipitation indicate that association of the ING subunit with JADE1-HBO1 is essential for growth inhibition and argue that ING tumor suppressor activity functions in part through the acetyltransferase activity of HBO1 within a p53-linked pathway. Our results provide important information on structural determinants responsible for assembly of functionally distinct MYST/ING HAT complexes from yeast to human cells. They unravel how different PHD finger domains within a single HAT complex cooperate to regulate functions in chromatin binding, transcription regulation, and control of cell proliferation, ultimately linking chromatin methylation and acetylation to the tumor suppression function of ING proteins.

MATERIALS AND METHODS

Cell culture, plasmids, and recombinant proteins. Tet-off retrovirus-transduced cell lines expressing FLAG-HBO1-TAP, FLAG-ING3-TAP, HA-ING4-TAP, and FLAG-ING5-TAP have been described previously (8). The JADE1L (L stands for long), JADE3, and human Eaf6 (hEaf6) full-length cDNAs were obtained from ORIGENE. For construction of hemagglutinin (HA)- or FLAG-tagged mammalian expression plasmids, full-length or truncated HBO1, JADE1/3, ING4/5, and hEaf6 were cloned by PCR into pcDNA3. For expression in bacteria, the different domains of JADE1, JADE3, ING4, ING5, HBO1, hEaf6, Yng2, and Esa1 were cloned by PCR into pGEX4T3 (GE Healthcare), pET15b+ (Novagen), or pST44 (55), and the recombinant proteins were purified following standard procedures. Mammalian expression vectors for HA- and FLAG-tagged JADE1S (S stands for short) with amino acids 1 to 509 [JADE1S(1-509)] isoform and its PHD mutants have been described previously (40). For transient transfections, 2×10^6 cells (HeLa S3, 293T, and RKO) were transfected with 8 μg of each expression plasmid by the calcium phosphate method. JADE1L/S and their PHD2 deletion mutants were cloned into the retroviral vector pRev-CMV-3×FLAG, and the retrovirus was used to transduce HeLa S3 cells. Expression levels for the different isolated clones were measured and found to be particularly low for JADE1L (data not shown). Details of the cloning procedures and primer sequences are available upon request. Nuclear localization of all transfected proteins was confirmed by immunofluorescence.

Antibodies and peptides. The following antibodies were used for Western blots: anti-FLAG M2-R (1:2,000) and anti-glutathione *S*-transferase (anti-GST) (1:2,000) (Sigma); anti-HA 3F10 (1:2,000) and 12CA5 (1:2000) (Roche); anti-6×His (1:4,000) (Clontech); anti-γH2AX (1:1,000) (Millipore); anti-H3 (1:10,000), antitubulin, anti-p21, anti-HBO1, anti-ING4, anti-ING5 (1:1,000), and anti-hEaf6 (1:500) (Abcam). Biotinylated histone peptides were kind gifts from Or Gozani (Stanford University) or purchased from Millipore.

Affinity purification of protein complexes. Tandem affinity purifications of native ING complexes from mammalian cells were done as previously described (8). For affinity purification from cotransfected cells, 293T cells were harvested 48 h posttransfection, washed twice with cold phosphate-buffered saline (PBS), and lysed in 1 ml/plate of lysis buffer (20 mM HEPES [pH 7.9], 150 mM KCl, 5% glycerol, 1 mM dithiothreitol [DTT], 100 μM Zn acetate, 2 mM $MgCl_2$, 2 mM EDTA, 0.2% [vol/vol] NP-40, 0.5 μg/ml aprotinin, 2 μg/ml leupeptin, 2 μg/ml pepstatin, 1 mM phenylmethylsulfonyl fluoride [PMSF], 0.1 mM Na_2MoO_4, 0.1 mM Na_3VO_4, 10 mM β-glycerophosphate, 10 mM NaF, and 10 mM Na butyrate) on ice for 30 min. The cell lysate was then clarified by centrifugation for 30 min at 21,000 × *g*. The supernatant was incubated for 3 h or overnight with FLAG-M2 agarose (Sigma) at 4°C. The resin was recovered by centrifugation and then washed five times with the same buffer but containing 0.1% (vol/vol) NP-40 and 300 mM KCl. Bound proteins were eluted with 400 ng/μl 3×FLAG peptide in elution buffer (20 mM HEPES [pH 7.5], 100 mM KCl, 0.1% Triton X-100, 5% glycerol). A portion of the eluate was resolved by SDS-PAGE and analyzed by Western blotting.

Peptide and GST pulldown assays. Concentrations of purified recombinant proteins were normalized by SDS-PAGE and Coomassie blue staining. The concentrations of biotinylated peptides were verified by antibiotin dot blots. For pulldown assays, 500 ng of biotinylated histone peptides was incubated with 1 μg of candidate binding protein in 100 μl of binding buffer (300 mM KCl, 50 mM Tris [pH 7.5], 0.05% [vol/vol] NP-40, 100 μg/ml bovine serum albumin [BSA], 1 mM PMSF) at 4°C for 3 h to overnight. After 1 h of incubation with streptavidin-coupled Dynabeads (Invitrogen), the beads were washed four times with binding buffer and subjected to a Western blot analysis with an anti-GST antibody. For GST pulldown assays, 500 ng of His-tagged proteins was precleared with glutathione Sepharose-bound GST and incubated with 1 μg of glutathione Sepharose-bound proteins in a final volume of 50 to 120 μl in pulldown buffer (25 mM HEPES [pH 7.5], 250 mM KCl, 10% glycerol, 100 μg/ml BSA, 0.1% [vol/vol] NP-40, 0.5 mM DTT, and protease inhibitors) for 2 h at room temperature. Supernatants were removed, and the resin was washed 2 times with pulldown buffer at 300 mM KCl and once with pulldown buffer at 150 mM KCl. Input (50%) and bound material were analyzed by Western blotting with anti-6×His antibodies.

HAT assays with protein complexes. Histone acetyltransferase (HAT) assays with histone peptides (300 ng) were performed essentially as described previously (66). Briefly, protein complexes were incubated with or without substrate in a final volume of 15 μl of 50 mM KCl, 50 mM Tris (pH 8), 1 mM DTT, 5% glycerol, 10 mM Na butyrate, and 0.1 mM EDTA with 0.5 μl of ^{3}H-labeled acetyl coenzyme A (acetyl-CoA) (0.25 μCi/μl; 4.9 Ci/mmol) for 45 min at 30°C. Each reaction mixture was spotted onto p81 filters, washed three times with 50 mM Na carbonate (pH 9.2), and processed for scintillation counting.

NMR spectroscopy. Nuclear magnetic resonance (NMR) experiments were performed at 25°C on Varian INOVA 600- and 500-MHz spectrometers using pulse field gradients to suppress artifacts and eliminate water signal. ^{1}H,^{15}N heteronuclear single quantum coherence (HSQC) spectra of uniformly ^{15}N-labeled JADE1 PHD1 and PHD-Zn knuckle-PHD (PZP) (0.1 to 0.2 mM) were recorded as histone tail peptides (synthesized by the University of Colorado at Denver [UCD] Biophysics Core Facility), and unlabeled PHD1 was added stepwise.

Microarray data analysis. Duplicate RNA samples from transduced HeLa cells stably expressing JADE1L were compared to samples from cells transduced with empty vectors. Four RNA samples (two independent experiments with duplicate samples for each) from siRNA-mediated knockdown of HBO1 (siHBO1)-treated HeLa cells (as described before [8]) were compared to samples from cells treated with control siRNA (luciferase). Illumina HumanHT-12 v3.0 and v4.0 microarray data were processed in BioConductor using the package lumi (31). The background corrected intensities from BeadStudio were directly imported into R (www.r-project.org) with the function lumiR. Data were first transformed to $\log_2$ and then normalized using quantile normalization using lumiT and lumiN functions, respectively. The test for statistical difference between the conditions was performed using the empirical Bayes method eBayes in limma (60). Multiple hypothesis correction was performed using the Benjamini-Hochberg correction. We considered a gene to be significantly differentially modulated between two conditions when the absolute $\log_2$ fold change is higher than $\log_2$ 1.5 and the adjusted *P* value is lower than 0.05.

Cell growth analysis. HeLa S3 cells retrovirally transduced to express JADE1 constructs were seeded at 4×10^4 cells per well of 6-well plates and allowed to grow in a standard tissue culture incubator. For each cell line, two independent wells were harvested on days 3, 5, and 7 postseeding. Cells were counted using an Auto T4 automated cell counter (Nexcelom Bioscience, Lawrence, MA).

Anchorage-independent cell growth. 1×10^5 HeLa S3 cells retrovirally transduced to express JADE1 constructs were suspended in Dulbecco modified Eagle medium (DMEM) containing 10% fetal bovine serum (FBS) and 0.3% agar and plated on 100-mm dishes in duplicate. Following 3 weeks of growth in a standard tissue culture incubator, four random fields on each plate were photographed using a light microscope with a magnification of ×4. Colonies in each field were counted using the AlphaImager software (Alpha Innotech, San Leandro, CA).

Assays of p53-dependent transcription. Reverse transcription-PCR (RT-PCR) assays were performed as described before (9). Luciferase reporter assays to test the capacity of ING4, HBO1, ING3, and Tip60 to potentiate p53-dependent transcriptional activation were performed in triplicate using the wwp/p21-luciferase reporter (10) and a pGL3-BAX-luciferase construct (Science Reagents Inc.) as previously described (8).

ChIP assays. Briefly, 2×10^8 asynchronously growing RKO cells were cross-linked with 1% formaldehyde followed by treatment with 125 mM glycine. The cells were then washed with PBS and resuspended in chromatin immunoprecipitation (ChIP) lysis buffer A (10 mM HEPES [pH 7.5], 10 mM EDTA, 0.5 mM EGTA, 0.75% Triton X-100) and incubated for 10 min on ice. The cells were then resuspended in ChIP lysis buffer B (10 mM HEPES [pH 7.5], 200 mM NaCl, 1 mM EDTA, 0.5 mM EGTA) and incubated on ice for 10 min. The cells were finally resuspended in ChIP lysis buffer C (150 mM NaCl, 25 mM Tris-HCl [pH 7.5], 0.1% SDS, 0.5% sodium deoxycholate, 1% Triton X-100, 1 mM PMSF, 2 μg/ml leupeptin, 5 μg/ml aprotinin, 2 μg/ml pepstatin) and sonicated on ice (Diagenode Bioruptor) to shear chromatin to an average length of 500 bp. After overnight incubation at 4°C using 1 mg of chromatin per IP with 5 μg of specific antibodies, protein A Dynabeads (Invitrogen) were added and incubated for 4 h at 4°C. The beads were washed extensively and eluted with 1% SDS and 0.1 M $NaHCO_3$. Cross-links were reversed overnight at 65°C in the presence of 0.2 M NaCl, and the samples were then treated first with RNase A and then with proteinase K. DNA was recovered using phenol-chloroform and ethanol precipitation. Quantitative real-time PCR was performed using SYBR green I (Roche) with LightCycler 480 (Roche). The error bars represent standard errors based on 3 independent experiments. Primers used in the PCRs (available upon request) were analyzed for linearity range and efficiency.

ChIP-seq analysis. Chromatin immunoprecipitation (ChIP) from RKO cells was done as described above. To prepare libraries for sequencing, DNA samples were processed with the Genomic DNA preparation kit (Illumina) according to the manufacturer's protocol. One microliter of adapter oligonucleotide mix (Illumina) was used for each ligation reaction. Gel-extracted DNA of each library was amplified through 18 PCR cycles. Samples were sequenced by 36-bp single reads on a Genome Analyzer II platform (Illumina). Raw sequences were mapped using BWA (29) on build hg18 of the human genome and deposited in the GEO database. Uniquely mapped sequences were kept for downstream analysis. The global profiles at transcription start sites presented in Fig. 8A were produced using the UCSC genome browser genes definition and the Python package HTseq. In the case of multiple TSS associated with the same gene, we selected the one with the highest number of HBO1 mapped reads within 5,000 bp around the transcription start site. We discarded genes transcribed in opposite directions for which TSS are at a distance lower than 10,000 bp to prevent introducing any artifacts in the global profiles. For gene expression level in RKO cells, we used publicly available data from an Affymetrix U133 plus 2.0 chip (70). The binning of genes by their function or level of expression was performed by first sorting the $\log_2$ expression level and then subdividing genes in four equal categories (quartiles).

Microarray and ChIP-seq data accession number. ChIP-seq raw data and microarray data and used in data analysis have been deposited in the GEO database under accession number GSE33221.

RESULTS

MYST-ING HAT complexes can be separated into three classes. On the basis of the available literature and our characterization of yeast and human MYST-ING HAT complexes, we identified three major conserved classes based on structure, sequence, and functional homologies (Fig. 1) (2, 4, 8, 9, 17, 63). We previously established yeast Piccolo NuA4 as a core tetrameric complex that encompasses strong nucleosomal HAT activity and also determined that the Epl1 protein assembles the complex by bridging the MYST enzyme Esa1 with the ING protein Yng2 (4, 55). After further analysis of MYST-ING complexes in eukaryotes, we suggested that they are all based on a similar tetrameric structure formed by homologous or related proteins (8). In this model, an Epl1-related factor independently interacts with MYST and ING proteins to assemble a functional complex (Fig. 1A). In support of this hypothesis, two short regions of sequence homology have been found in the scaffold subunits of all MYST-ING complexes (boxes labeled I and II in Fig. 1B; see the sequences in Fig. 3A), suggesting that these are the binding regions for MYST and ING proteins (8). To test this hypothesis, we performed *in vivo* and *in vitro* interaction studies, focusing our efforts on the human HBO1 complex.

JADE proteins coordinate the assembly of HBO1 complexes. JADE1, a candidate tumor suppressor, has been physically linked to von Hippel-Lindau (VHL) function, transcription regulation, Wnt signaling, and apoptosis (6, 40, 74–76). Our initial purification of HBO1 acetyltransferase complexes identified full-length JADE1/2/3 paralogues as stably associated subunits (8). Subsequently, it became clear that HBO1 could also associate with a shorter isoform of JADE1, named JADE1S (Fig. 2A) (12, 53). In fact, the bulk of functional information on JADE1 in the literature is based on this smaller 509-amino-acid protein produced by an abundant mRNA splice variant (40, 74–76).

To confirm the role of JADE1 as the scaffold of the complex, we first verified that there was no direct interaction between HBO1 and ING proteins by performing cotransfections and immunoprecipitations followed by Western blot analyses (data not shown). We then produced N-terminal and C-terminal deletions of JADE1L and analyzed their assembly into complexes by simultaneous cotransfections with HBO1 and ING5 (Fig. 2B). Analysis of immunopurified JADE1 indicates that association with ING5 requires amino acids 509 to 600 of JADE1L that encompass a portion of the conserved domain II (Fig. 2B, lane 2 versus lane 3). In contrast, the interaction between HBO1 and JADE1 depends primarily on domain I contained within amino acids 114 to 199 (lane 5 versus 6). Similar results were obtained using ING4 instead of ING5 and the JADE3 paralogue (data not shown). Thus, JADE1L functions as the scaffold of the HBO1 complex by performing direct and independent interactions with the ING and HBO1 proteins *in vivo*, through regions containing conserved domains I and II (Fig. 1B and 2A). These data also confirm that the shorter JADE1S isoform does not associate with ING proteins *in vivo* (12, 53).

We then analyzed the requirements for the association of the fourth subunit of HBO1 complexes, hEaf6. This protein is present in all MYST-ING HAT complexes, but its role is unknown.

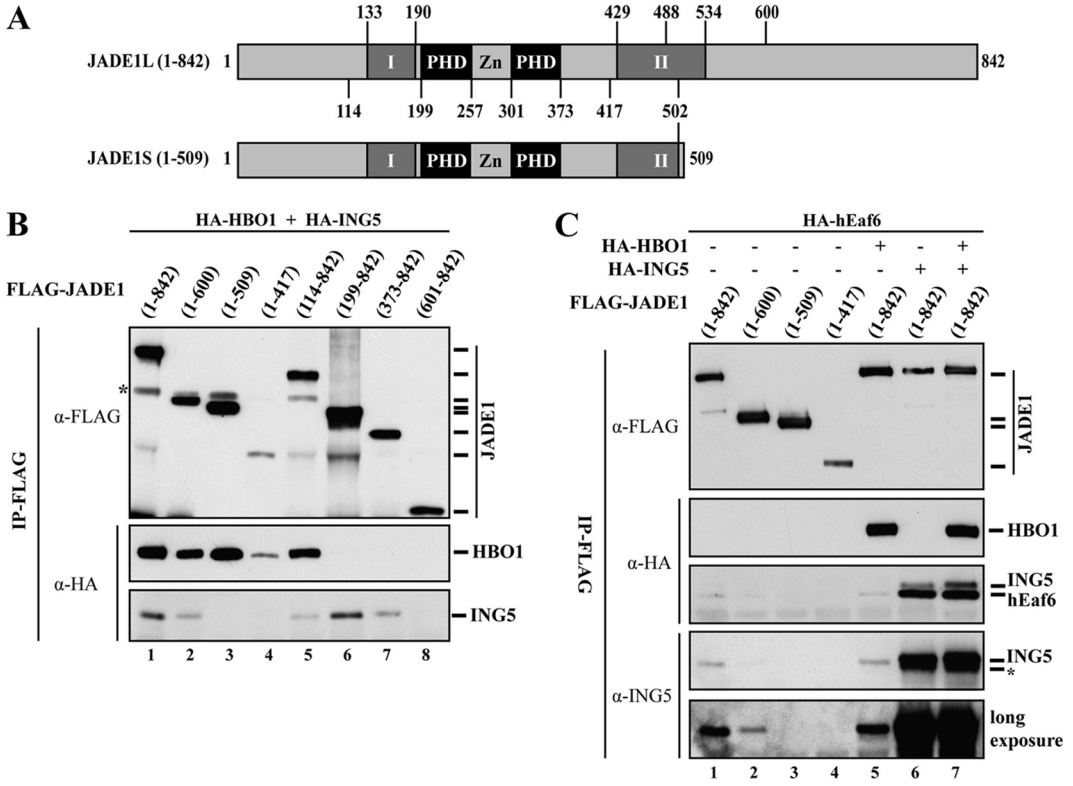

FIG 2 Molecular determinants for assembly of HBO1 HAT complexes. (A) Schematic representation of JADE1 protein isoforms produced by mRNA splice variants. The numbers are amino acids. (B) Distinct regions of JADE1 are required for HBO1 and ING5 interaction. Indicated N-terminal and C-terminal deletion mutants of FLAG-JADE1 were affinity purified after cotransfection with HA-HBO1 and HA-ING5 and analyzed by Western blotting. JADE1(1-509) corresponds to the JADE1S natural isoform. The numbers within parentheses above the lanes are the amino acid positions [e.g., (1-842), amino acids 1 to 842]. α-FLAG, anti-FLAG antibody. (C) Stable association of hEaf6 with JADE1 requires ING5. FLAG-JADE1 coimmunoprecipitations were analyzed as described after cotransfections with the indicated vectors. Asterisks indicate residual HB01 (B) and hEaf6 (c) signals.

Cotransfections show a clear association of hEaf6 with HBO1/JADE1L/ING5 (Fig. 2C, lane 7). The interaction of hEaf6 with the complex is greatly enhanced by the presence of ING5 in an HBO1-independent manner (Fig. 2C, lanes 1 and 5 versus lanes 6 and 7). However, no direct interaction was detected between ING4/5 and hEaf6 by cotransfection (data not shown). These results argue that, like ING5 and HBO1, hEaf6 binds JADE1, but its interaction with the scaffold protein requires the presence of ING5. We speculate that the presence of small amounts of HA-hEaf6 with JADE1 immunopurified in the absence of cotransfected ING5 (Fig. 2C, lane 1) is mediated by the endogenous ING5 protein, which can be detected in the immunoprecipitations with an anti-ING5 antibody after a long exposure (Fig. 2C).

Overall, our current and previously published analyses indicate that each MYST-ING complex contains a scaffold subunit that appears to make independent interactions with the MYST HAT enzyme and the ING proteins (Fig. 1 and 2 and data not shown) (4, 9, 12, 65).

Short domains conserved in all MYST-ING complexes are responsible for bridging specific acetyltransferases with their ING factors. To map more precisely the interactions detected in the HBO1 complexes and to address directly the roles of conserved domains I and II of JADE1, we performed glutathione *S*-transferase (GST) pulldown assays using recombinant polypeptides. Domains I and II of JADE1L (Fig. 3A) were fused to GST and tested for interaction with HBO1, ING4, and hEaf6. In agreement with the model proposed above, we found that ING4 shows strong specific binding to domain II, while HBO1 interacts with domain I (Fig. 3B). These interactions occur through the HBO1 MYST domain (Fig. 3B, middle panel), and independently of the ING4 PHD finger (Fig. 3B, bottom panel). We then tested the determinants for hEaf6 association. No binding was observed between hEaf6 and domain I of JADE1 (Fig. 3C, top panel). A very weak interaction could be detected between hEaf6 and domain II of JADE1 (Fig. 3C, top panel), and it was greatly enhanced by the addition of ING4 to the reaction mixture (Fig. 3C, bottom panel), reminiscent of what we observed *in vivo* (Fig. 2C). Again, no interaction between hEaf6 and ING4 could be detected in the absence of JADE1 domain II.

On the basis of domain II sequence homology between JADE, BRPF, EPC, yeast Epl1 (yEpl1), and yNto1 proteins, we can identify two subdomain regions separated by a short linker, labeled here IIa and IIb (Fig. 3A). Pulldown assays using both domains and recombinant ING4 show a specific and strong interaction with domain IIb and none with IIa (Fig. 3D). Critically, as indicated in Fig. 3A, domain IIb is disrupted in the JADE1S splice variant, which accounts for this isoform's inability to bind ING proteins (Fig. 1B) (10, 43).

Altogether, these results clearly demonstrate the role of JADE1 as a platform for assembly of HBO1 complexes through distinct molecular interactions with each subunit. They also confirm our hypothesis that two small peptide regions conserved in a specific

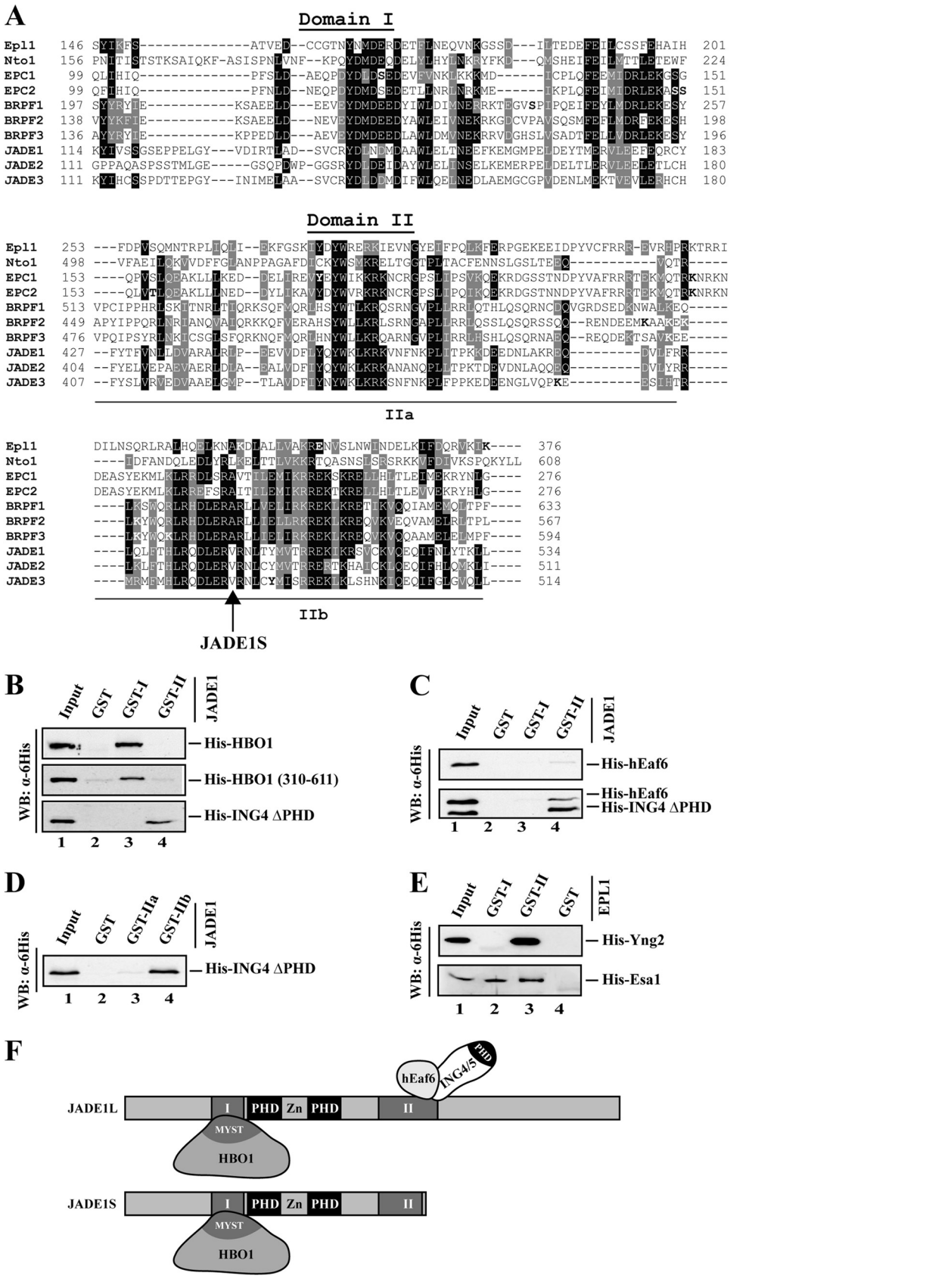
A
Domain I
Epl1 146 SYIKFS--------------ATVEP--CCGTNYNMDERDETFLNEQVNKGSSD---ILTEDEFEILCSSFEHAIH 201
Nto1 156 PNITISTSTKSAIQKF-ASISPNLVNF--KPQYDMDEQDELYLHYLNKEYFKE---QMSHEIFELMTTLETEWF 224
EPC1 99 QLIHIQ--------------PFSLD--AEQPDYDLDSEDEVEVNKLKKKMD------ICPLQFEEMIDRLEKGSG 151
EPC2 99 QFIHIQ--------------PFNLD--NEQPDYDMDSEDETLLNRLNRKME------IKPLQFEIMIDRLEKASS 151
BRPF1 197 SYYRYIE-----------KSAEELD---EEVEYDMDEEDYIWLDIMNERRKTEGVSPIPQEIFEYLMDRLEKESY 257
BRPF2 138 VYYKFIE-----------KSAEELD---NEVEYDMDEEDYAWLEIVNEKRKGECVPAVSQSMFEFLMDRFEKESH 198
BRPF3 136 AYYRYIE-----------KPPEDLD---AEVEYDMDEEDLAWLDMVNEKRRVEGHSLVSADTFELLVDRLEKESY 196
JADE1 114 KYIVSSGSEPPELGY---VDIRTLAD--SVCRYDLNDMDAAWLELTNEEFKEMGMPELDEYTMERVLEEFEQRCY 183
JADE2 111 GPPAQASPSSTMLGE-----GSQPEWP-GGSRYDLDEIDAYWLELINSELKEMERPELDELTLERVLEELETLCH 180
JADE3 111 KYIHGSSPDTTEPGY---INIMELAA--SVCRYDLDDMDIFWLQELNEDLAEMGCGPVDENLMEKTVEVLERHCH 180
Domain II
Epl1 253 ---FDFVSQMNTRPLIQLI--EKFGSKIYDYWREKIEVNGYEIFPQLKFERPGEKEEIDPYVCFRRR-EVRHFRKTRRI 326
Nto1 498 ---VFAEILCKVVDFFGLANPPAGAFDICKYWSMKRELTGGTPLTACFENNSLGSLTEEQ----------VQTR----- 561
EPC1 153 ----QPVSLQEAKLLLKED--EELIREVYEYWIKKRKNCRGPSLIPSVKQEKRDGSSTNDPYVAFRRRTFKMQTRKNRKN 226
EPC2 153 ----QLVTLQEAKLLLNED--EYLIKAVYDYWVRKRKNCRGPSLIPQIKQEKRDGSTNNDPYVAFRRRTFKMQTRKNRKN 226
BRPF1 513 VPCIPPHRLSKITNRLTQRKSQFVQRLHSYWTLKRQSRNGVPLLRRLQTHLQSQRNCDQVGRDSEDKNWALKEQ----- 586
BRPF2 449 APYIPPQRLNRIANQVAQRKKQFVERAHSYWLLKRLSRNGAPLLRRLQSSLQSQRSSQQ--RENDEEMKAAKEK----- 522
BRPF3 476 VPQIPSYRLNKICSGLSFQRKNQFVQRLHNYWLLKRQARNGVPLLRRLHSHLQSQRNAEQ--REQDEKTSAVKEE----- 549
JADE1 427 --FYTFVNLLDVARALRIP--EEVVDFLYQYWKLKRKVNFNKPLITPKKDEEDNLAKREQ---------DVLFRR----- 490
JADE2 404 --FYELVEPAEVAERLDIA--EALVDFIYQYWKLKRKANANQPLLTPKTDEVDNLAQQEQ---------DVLYRR----- 467
JADE3 407 --FYSLVRVEDVAAELGVP--TLAVDFIYNYWKLKRKSNFNKPLFPPKEDEENGLVQPKE---------ESIHTR----- 470
IIa
Epl1 DILNSQRLRALHQELKNAKDLALLVAKRENVSLNWLNDELKIFDQRVKIK---- 376
Nto1 ----IDFANDQLEDLYRLKELTTLVKKRTQASNSLSKSRKKVFDIVKSPQKYLL 608
EPC1 DEASYEKMLKLRRDLSRAVTILEMIKRREKSKRELLHITLEIMEKRYNLG---- 276
EPC2 DEASYEKMLKLRREFSRAITILEMIKRREKTKRELLHITLEVVEKRYHLG---- 276
BRPF1 ----LKSWQRLRHDLERARLLVELIRKREKLKRETIKVQQIAMEVQLTPF---- 633
BRPF2 ----LKYWQRLRHDLERARLLIELLRKREKLKREQVKVEQVAMELRLTPL---- 567
BRPF3 ----LKYWQKLRHDLERARLLIELIRKREKLKREQVKVQQAAMELELMPF---- 594
JADE1 ----LQLFTHLRQDLERVRNLTYMVTRREKIKRSVCKVQEQIFNLYTKLL---- 534
JADE2 ----LKLFTHLRQDLERVRNLCYMVTRRERTKHAICKLQEQIFHLQMKLI---- 511
JADE3 ----MRMFMHLRQDLERVRNLCYMISRREKLKLSHNKLQEQIFGLGVQLL---- 514
IIb
JADE1S
B
Input
GST
GST-I
GST-II
JADE1
WB: α-6His
His-HBO1
His-HBO1 (310-611)
His-ING4 ΔPHD
1 2 3 4
C
Input
GST
GST-I
GST-II
JADE1
WB: α-6His
His-hEaf6
His-hEaf6
His-ING4 ΔPHD
1 2 3 4
D
Input
GST
GST-IIa
GST-IIb
JADE1
WB: α-6His
His-ING4 ΔPHD
1 2 3 4
E
Input
GST-I
GST-II
GST
EPL1
WB: α-6His
His-Yng2
His-Esa1
1 2 3 4
F
hEaf6
ING4/5
PHD
JADE1L
I
PHD
Zn
PHD
II
MYST
HBO1
JADE1S
I
PHD
Zn
PHD
II
MYST
HBO1

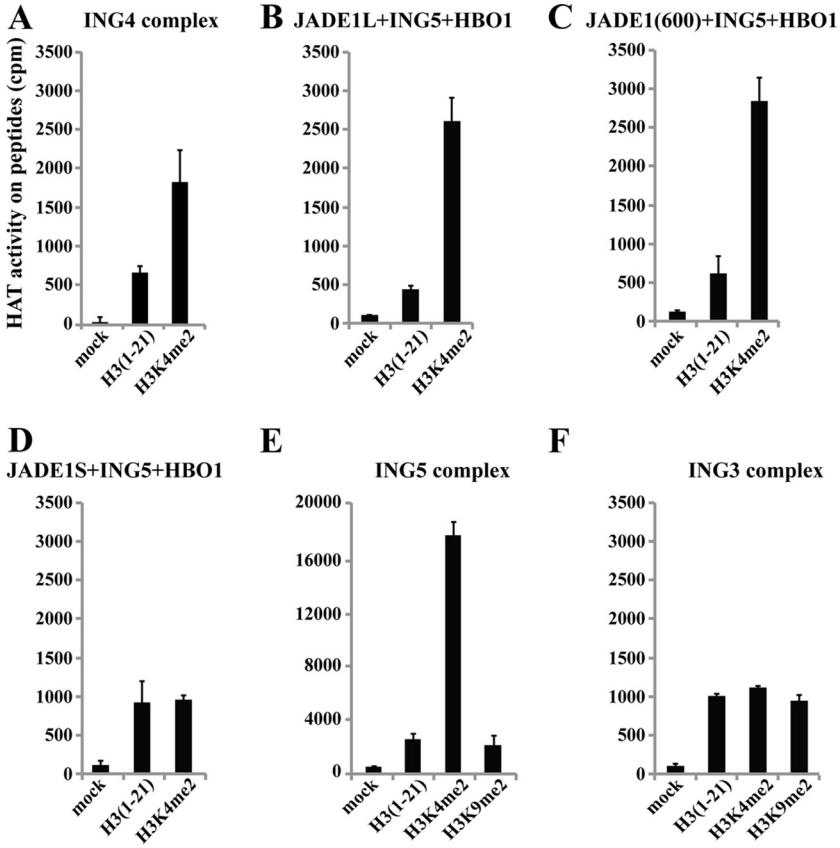

FIG 4 Domain II-dependent association of ING subunits stimulates MYST HAT activity toward histone H3 peptides methylated on lysine 4. (A) Native ING4 complex preferentially acetylates histone H3 tails that are methylated on lysine 4. Purified native ING4 complex (ING4, JADE, HBO1, and hEaf6 [Fig. 1A]) was tested in HAT assays with the indicated histone H3 peptides. Reactions were spotted on membranes and counted by liquid scintillation. (B to D) Domain IIb-dependent physical association of the ING subunit is required for stimulation of HBO1 HAT activity on H3K4me tails. HBO1 HAT was affinity purified after cotransfection with the indicated cDNAs and tested in HAT assays on peptides as described above for panel A. (E and F) Stimulation of H3 acetylation by H3K4me is seen only with H3-specific HATs. Purified native ING5 (a mix of HBO1 and MOZ/MORF complexes [Fig. 1A]) and ING3 (Tip60) acetyltransferase complexes were tested as described above for panel A.

subunit of all MYST-ING complexes are responsible for bridging together MYST HATs and ING proteins. These conserved interactions were also confirmed using domains I and II of the Epl1 subunit of the yeast Piccolo NuA4 complex (Fig. 3E) and are corroborated by our previous cotransfection experiments with human MOZ-BRPF1-ING5 complex (65). Furthermore, the natural occurrence of an abundant splice variant of JADE1 producing a shorter isoform (74) represents a mechanism of regulating the association of ING4/5 proteins with the HBO1 HAT, supporting the concept of functionally distinct roles of HBO1 complexes with or without an ING subunit (Fig. 3F; see below).

Domain II-mediated association of ING proteins with JADE-HBO1 determines the modulation of acetyltransferase activity by methylated lysine 4 of histone H3. A hallmark of ING tumor suppressor proteins is the presence of a C-terminal PHD finger domain. This domain in ING proteins has been shown to specifically interact with histone H3 methylated at lysine 4 (5, 18, 33, 41, 53, 56, 63). This association has an impact on HAT activity of MYST-ING complexes as shown by HAT assays using purified native ING4-HBO1-JADE-hEaf6 complex with histone H3 tail peptides unmodified or methylated on lysine 4 (H3K4me). We observed that the acetyltransferase activity of the ING4 complex is strongly stimulated by methylation of lysine 4 (Fig. 4A). To delineate the determinants of this stimulation, we purified HBO1-JADE1-ING5 following transient transfection and observed that the HAT activity of this complex was similarly stimulated by H3K4me (Fig. 4B). Interaction of ING5 with domain IIb of JADE1 was specifically required for this stimulation, as JADE1(1-600),

FIG 3 Molecular dissection of MYST-ING HAT complexes identifies two conserved domains essential for assembly. (A) Sequence alignment of conserved domains in yeast and human proteins associated with ING/MYST-containing HAT complexes. Domain II can be further subdivided into two parts based on concentrations of homology. The location of the frameshift removing the C-terminal portion of domain II in JADE1S is shown. Sites of posttranslational modifications are indicated in boldface type. (B to D) ING4 binds JADE1 domain IIb *in vitro*, while HBO1 interacts with domain I, and hEaf6 needs ING4 to efficiently associate with JADE1 domain II. GST pulldown assays with the indicated recombinant proteins were analyzed by Western blotting (WB). HBO1 amino acids (aa) 310 to 611 [HBO1 (310-611)] represents the carboxyl terminus of the protein containing the MYST domain. ING4 ΔPHD includes aa 1 to 169 of the protein. (E) The functions of domains I and II are conserved in other MYST-ING complexes. GST pulldowns as described above for panel D using homologous domains in yeast Epl1 with Esa1 MYST and Yng2 ING proteins. (F) Model of interactions within HBO1 complexes and the effect of the JADE1S shorter isoform.

but not JADE1S(1-509), displayed increased acetylation of H3K4me peptides (Fig. 4C and D). Similarly, a BRPF1-dependent association of the MOZ/MORF complexes with ING5 was required to observe increased acetylation in response to H3 K4 methylation (5). Native purified ING5 complexes (a mix of HBO1-JADE and MOZ/MORF-BRPF complexes [7]) also showed a very strong stimulation of HAT activity by H3K4me, while their activity remained unchanged in response to methylation of H3 on lysine 9 (Fig. 4E). On the other hand, this effect was not seen with the native ING3 complex (large Tip60-EPC complex) (Fig. 4F), likely reflecting the fact that histone H3 is not a physiological target of the Tip60 MYST enzyme (8, 9). Taken together, these results support a role for the ING subunits in stimulating the activity of MYST HAT complexes toward H3 K4me-containing chromatin, a mark highly enriched around transcription start sites of active genes.

MYST-ING4/5 HAT complexes contain multiple histone H3-binding PHD finger domains with different specificities toward lysine 4 methylation status. As shown in Fig. 1B, MYST-ING HAT complexes contain multiple domains that are potentially important for protein-protein interactions and for binding to specific chromatin regions. Interestingly, ING4/5 complexes contain other PHD finger domains in addition to the one in the ING proteins. We have previously shown that JADE PHD domains display striking specificities (53). While the second PHD of the PHD-Zn knuckle-PHD (PZP) region binds the H3 N-terminal tail irrespective of its methylation status, the first domain (PHD1) binds the same portion of H3 only when H3K4 is not methylated. A similar property of the first PHD finger of BRPF2 was recently reported (44). We confirmed these binding properties of PHD1 and PHD2 of JADE1 and JADE3 in peptide pulldown experiments using recombinant domains fused to GST and biotinylated peptides (Fig. 5A). While we have previously demonstrated that the histone H3 tail and PHD2 of JADE1 were critical for HBO1 association with chromatin *in vitro* and *in vivo*, we have also shown that PHD1 has a dominant effect within the PZP domain and in the absence of associated ING proteins blocks the interaction with H3 tails methylated on lysine 4 (12, 53). The dominance of PHD1 within the PZP domain was further underlined by NMR analysis of binding to H3 peptides, showing similar chemical shift changes with each construct (Fig. 5B). Such significant chemical shift changes could not be obtained with PHD2 alone, as it did not seem properly folded for NMR analysis. These results lead us to suggest that the PZP domain functions as a single functional entity for interaction with chromatin and that our previous results obtained with PHD2 deletion mutant in fact reflect disruption of the entire PZP structure (53).

This observation raises interesting questions regarding the putative cross talk between chromatin and these modules and their ability to functionally regulate MYST-ING complex localization in the genome. It also suggests that such interactions could regulate HAT activity of the complexes and underlines the potential impact of controlling the ING subunit association with the complex.

Association of the ING proteins with HBO1-JADE is required for growth control. We have previously shown that transduced clones of HeLa cells expressing full-length JADE1L protein grew very slowly in normal conditions, while the protein unable to bind chromatin due to mutated PHD2 had no effect on growth (53). This is clearly linked to the proposed tumor suppressor activity of JADE1 (74), since anchorage-free growth measured by colony formation in soft agar is also decreased by JADE1L but not the mutant (53). However, it was still important to determine whether this growth inhibition effect required an association with ING tumor suppressor proteins. As shown in Fig. 6A and B, stable expression of the JADE1S isoform, incapable of interacting with ING4/5 but still associated with HBO1, has no significant effect on normal cell growth or anchorage-free colony formation. The stable clones expressing JADE1L were difficult to maintain in culture, as they tend to undergo growth arrest after several passages. This behavior was linked to the level of JADE1L expression but was still seen even when the protein was expressed at a lower level than in other constructs (data not shown), suggesting that even a slight disruption of the balance between HBO1 complex subunits can have a profound effect on cell viability.

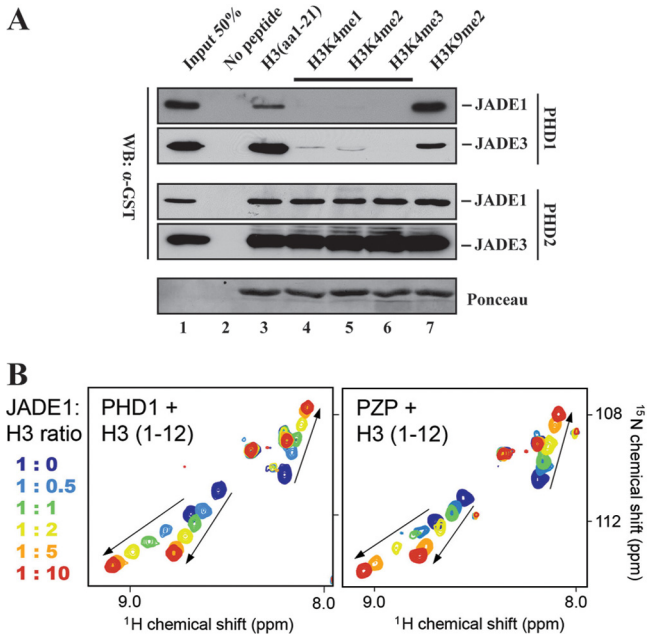

FIG 5 The first PHD finger of the JADE1 PZP domain dictates the specificity of the entire domain toward histone H3K4 methylation status. (A) JADE PHD finger domains interact with histone H3 tail peptides *in vitro*, but with different effect of lysine 4 methylation. Peptide pulldown assays with the indicated biotinylated peptides and recombinant PHD fingers fused to GST were analyzed by Western blotting with anti-GST (WB:α-GST). JADE PHD1s prefer the nonmethylated form, while PHD2s bind H3 peptides in a methylation-independent manner. H3 K9 methylation has limited effect on the binding of these PHD fingers. (B) NMR analysis indicates that JADE1 PHD1 alone binds the H3 tail similarly to the full PZP domain. Superimposed ^{1}H,^{15}N HSQC spectra of JADE1 PHD1 and PZP, recorded during the addition of the indicated H3 peptides. The spectra are color coded according to the protein-peptide ratio.

It was interesting to determine whether this slow growth phenotype was linked in some way to a cell cycle checkpoint activation, genome instability, and/or cell death. Western blot analyses indicated that JADE1L-expressing cells possess a higher level of endogenous γH2AX (Fig. 6C), a mark linked to DNA damage and checkpoint activation that could also reflect DNA fragmentation during cell death (3). We then measured the expression of genes in JADE1L-transduced cells using DNA microarrays. Over 499 genes were found to be significantly upregulated when JADE1L was expressed compared to cells transduced with the empty vector, while

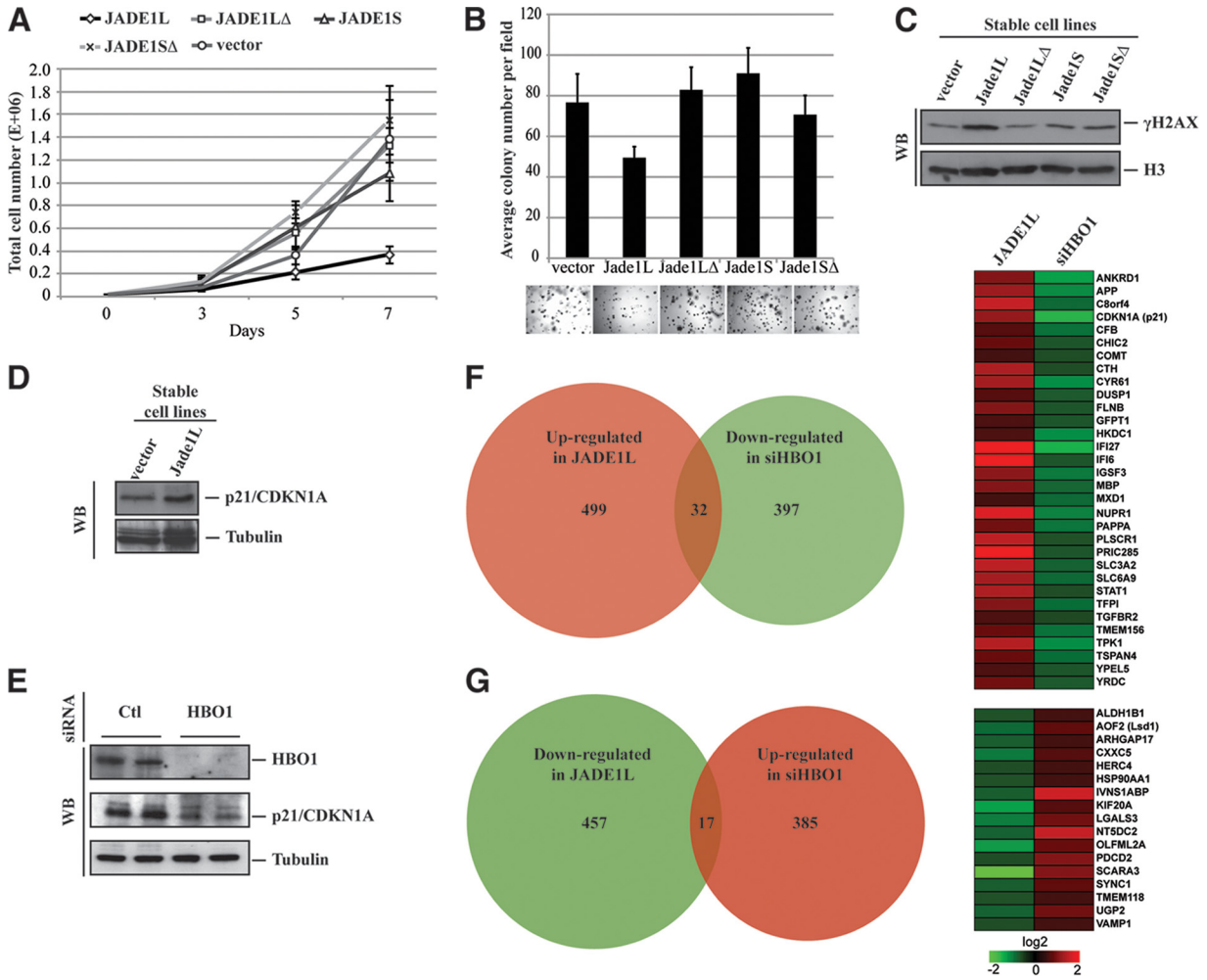

FIG 6 JADE1 interaction with ING is essential for tumor suppressor activity which implicates HBO1-dependent upregulation of the p21 CDK inhibitor. (A) Expression of JADE1L strongly inhibits HeLa cell growth, while JADE1S or PHD-deleted mutants do not. Indicated transduced cell lines were seeded at the same density, and cells were counted over a period of 7 days. (B) JADE1L inhibits anchorage-independent cell growth, while JADE1S or PHD-deleted mutants do not. HeLa cell clones expressing the different constructs were grown in soft agar for 3 weeks, and colony formation was measured. Examples of image fields are shown below the bars in the graph. (C) JADE1L-expressing cells contain higher levels of γH2AX, a marker of DNA damage response, cell cycle checkpoint activation, and senescence. Whole-cell extracts of the indicated JADE1-expressing clones were analyzed by Western blotting with the indicated antibodies. (D and E) JADE1L expression increases p21 protein level, while HBO1 depletion decreases it. Western blot as in panel C, using p21 and tubulin antibodies on the indicated transduced or knocked-down HeLa cells. (F and G) Venn diagrams showing the number of genes significantly up- or downregulated by JADE1L expression or HBO1 depletion, and the genes commonly affected but in opposite ways (fold change of >1.5 with P value < 0.05).

457 genes were downregulated (see Table S1 in the supplemental material). Examples of genes significantly affected are presented in Table 1. Among the upregulated genes were a large number of interleukins, which have a well-established link to cellular senescence (1, 16, 24, 48, 49), as well as the STAT1 transcription factor. In addition, genes linked to or regulated by the p53 pathway were also upregulated, most strikingly, the p21/WAF1 cyclin-dependent kinase (CDK) inhibitor. Increased amounts of the p21 gene product were also confirmed by Western blotting (Fig. 6D). These results suggested that growth inhibition by JADE1L expression may occur through a p53-related pathway involving the well-known p21 CDK inhibitor, which has been linked to cell cycle arrest in response to DNA damage, cellular senescence, and apoptosis (21).

HBO1 depletion leads to downregulation of multiple genes in the p53 pathway of cell cycle control and apoptosis. In order to identify genes that are regulated by HBO1-JADE complexes *in vivo*, we used microarrays to measure gene expression after siRNA-mediated knockdown of HBO1 (siHBO1) in HeLa cells in comparison to a control small interfering RNA (siRNA) (see Table S2 in the supplemental material). Examples among the 397 genes that were upregulated and 385 genes that were downregulated are presented in Table 2. It is striking to see the number of p53-regulated genes that are repressed during HBO1 depletion, including not only p21/CDKN1A but also several others implicated in apoptosis. Knockdown of HBO1 and the associated decrease of the p21 protein were confirmed by Western blotting (Fig. 6E). It is also important to note that many genes important for transcription repression and heterochromatinization were upregulated during HBO1 knockdown, including H3K4 demethylase-, histone deacetylase-, and DNA methyltransferase-associated factors.

If a gene is directly regulated by the HBO1-JADE-ING com-

TABLE 1 Examples of genes affected during stable expression of JADE1L in HeLa cells[a]

Category	Genes[b]
Downregulated genes	CCNM2, DAB2[c], p57/KIP2/CDKN1C, p18/INK4C/CDKN2C , H19; SAP30[d], LSD1/AOF2/BHC110/KDM1A[d], CDK5, 14-3-3 sigma[e], MCM5, DMAP1[d], GMNN, CCNF and SKP2, and CCNE1 and CCNB1 genes
Upregulated genes	GDF15[e]; IL-1A/B, IL-6, IL-8, IL-24, and IL-32[f]; CCND1; JUN; VEGFA; CDK7 (TFIIH); STAT1; p21/WAF1/CDKN1A[e,f]; DNase II; GADD45A[e]; GADD45B[e]; APP[e]; IGF2BP2[e]; and p8/NUPR1[e] genes

[a] See Table S1 in the supplemental material for the full list of genes whose expression is significantly affected in transduced HeLa cells expressing JADE1L (>1.5-fold change [up or down] with P value of <0.05).
[b] IL-1A/B, interleukin 1A or B; VEGFA, vascular endothelial growth factor A.
[c] Linked to the Wnt signaling pathway.
[d] Linked to chromatin-mediated repression or heterochromatin formation (deacetylation, H3K4 demethylation, DNA methylation).
[e] Linked to or regulated by the p53 pathway.
[f] Linked to cellular senescence.

TABLE 2 Examples of genes affected during HBO1 depletion by siRNA in HeLa cells[a]

Category	Genes
Downregulated genes	DUSP2[c], NKD2[d], CASP9[c], p21/WAF1/CDKN1A[c], NEDD4[c], p18/INK4C/CDKN2C APP[c], BAX[c], HOXA10, IGFBP3[c], p8/NUPR1[c], EXT2, CDK11, MAD, BAG1[c], APAF1[c], CASP3[c], PTEN[c], FOS, STAT1, STAT5, DKK[d], and PIM1[c] genes
Upregulated genes	MAPK3/ERK1, 14-3-3 eta, KAP1/CDKN3[c], YES1, HMGN4, MSX1, LCOR[e], HOXA5, POLD3, DNMT1[e], BID[c], FZD4[d], FZD9[d], LSD1/AOF2/BHC110/KDM1A[e], BHC80/PHF21A[e], UHRF1[e], HELLS/LSH[e], TLE4[e], BRMS1L[e], TRIM24/TIF1alpha[c], TRIM33/TIF1gamma[e], BRPF1, and BCL9[d] genes

[a] See Table S2 in the supplemental material for the full list of genes whose expression is significantly affected in HeLa cells after siRNA-mediated knockdown of HBO1 (>1.5-fold change [up or down] with P value of <0.05).
[b] MAPK3, mitogen-activated protein kinase 3; ERK1, extracellular signal-regulated kinase 1.
[c] Linked to or regulated by the p53 pathway.
[d] Linked to the Wnt signaling pathway.
[e] Linked to chromatin-mediated repression or heterochromatin formation (deacetylation, H3K4 demethylation, DNA methylation).

plexes, one would expect its expression to be inversely affected in JADE1L-overexpressing cells versus HBO1-depleted cells. Results from the two sets of microarray experiments were compared to find such genes, and these genes are presented in Fig. 6F and G. While the number of genes that fit this criteria is limited, p21/CDKN1A and the LSD1/KDM1A H3K4 demethylase are among those showing this pattern of misregulation in JADE1L versus siHBO1 cells. These results suggest that the p21 gene could be a direct target of the HBO1-JADE-ING complexes through local recruitment and acetylation.

Growth control by the HBO1-JADE1L-ING complex occurs through direct recruitment and action at p53-regulated genes. As for JADE1L, increased expression of ING proteins in transduced HeLa cells leads to decreased colony formation in soft agar, a characteristic of tumor suppressors (Fig. 7A). Overexpression of the different components of the HBO1 complex during transient transfections also leads to increased transcription of the p21/CDKN1A gene, as measured by RT-PCR (Fig. 7B). JADE1S has less effect under these conditions, presumably because of its lack of interaction with ING proteins. Since HeLa cells are known to possess a compromised p53 pathway due to the presence of the HPV E6 protein that targets it for degradation, we carried out subsequent experiments in the p53-positive RKO cells from human colon carcinoma, since these cells have been used extensively in the initial studies of ING proteins (38, 39, 58). Using a luciferase reporter gene under the control of the p21 promoter, we were able to show that expression of the ING3 and ING4 proteins leads to increased transcription from p21, as previously reported (39, 58) (Fig. 7C). Furthermore, the cotransfection of a short hairpin RNA (shRNA) vector targeting p53 highlights the dependence of the ING-mediated stimulation of the p21 promoter activation on p53. Expression of HBO1 shows an even stronger effect than that of its associated ING4 subunit, and this effect is again lost upon p53 depletion. By comparison, expression of the ING3-associated Tip60 acetyltransferase, a known regulator of the p53 pathway (2), has a small effect. This suggests that ING3 augments the activity of this promoter by a mechanism that does not involve recruitment of the Tip60 HAT activity. These outcomes can be also detected using a different p53-regulated promoter, BAX, although overall expression and stimulation in this case are weaker (Fig. 7D). Finally, to determine whether the HBO1-JADE-ING complexes directly regulate p53-dependent transcription of the p21 gene, we performed chromatin immunoprecipitation (ChIP) experiments using polyclonal antibodies against HBO1 and ING5 proteins. As shown in Fig. 7E, both proteins are clearly enriched *in vivo* around the transcription start site (TSS) of the p21 gene, a region of chromatin particularly dense in histone H3 methylated at lysine 4, which serves as the binding target of the ING4/5 PHD fingers. Altogether, these results indicate that the HBO1-JADE1L-ING4/5 complexes control cell growth in part through direct binding and activation of the p21/CDKN1A promoter in a process that is mediated by p53.

HBO1 is located in the 5′ region of transcribed genes and colocalizes with H3K4me3. In order to precisely map the localization of native HBO1 complexes throughout the genome, we performed a ChIP-seq experiment in RKO cells. Analysis of ChIP-seq signal unveiled that genome-wide, HBO1 is mainly located immediately downstream of the TSS of genes and that its signal intensity strongly correlates with gene expression level (Fig. 8A). We also saw a significant enrichment of HBO1 over promoter regions within the 2 kb upstream of the transcription start site, with a diminished occupancy at the TSS itself. A more detailed analysis over the HOXA cluster indicated a strong enrichment of HBO1 mostly near the HOXA9 and HOXA10 genes (Fig. 8B). This observation is of interest, as expression of HOXA10 was found to be downregulated upon knockdown of HBO1 in our microarray experiment (Table 2). Finally, localization of HBO1 at the p21 locus demonstrated exactly the pattern described above, with the highest enrichment within the first 3 kb of the coding region of the

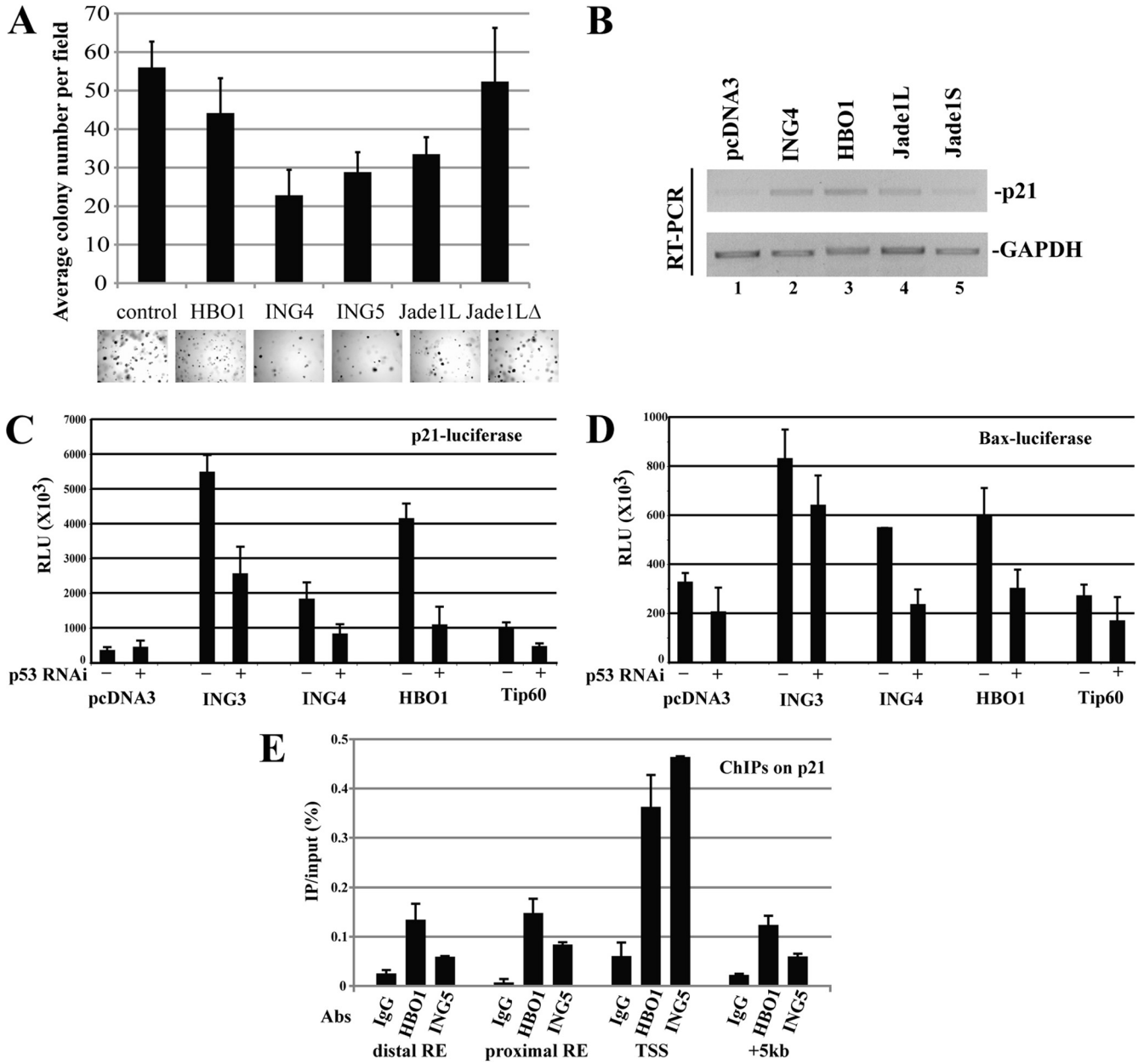

FIG 7 HBO1-JADE-ING complexes directly bind and stimulate p53-regulated genes to control cell proliferation. (A) HBO1-JADE1L-ING4/5 inhibits anchorage-independent cell growth. HeLa clones expressing the different constructs were incubated in soft agar, and colony formation was measured as described in the legend to Fig. 6B. (B) Overexpression of HBO1, JADE1L, and ING4 increases endogenous p21 transcription. RT-PCR analysis of HeLa cells transfected with the indicated expression vectors. GAPDH, glyceraldehyde-3-phosphate dehydrogenase. (C and D) HBO1 and ING4 proteins stimulate p53-dependent transcription. Luciferase assays on RKO cells transfected with the indicated expression vectors. The cells were also transfected with a shRNA expression vector against p53 or control (empty). Luciferase reporters tested were under the control of the p21 (C) or BAX (D) promoters. Data from triplicate cultures are presented with standard deviations (error bars). RLU, relative light units; RNAi, RNA interference. (E) HBO1-ING complex is bound to the p21 promoter *in vivo*, near the transcription start site (TSS). ChIP analysis of HBO1 and ING5 enrichment on the p21/CDKN1A gene. Values representing direct IP over the input ratio are based on three different cultures with standard errors. RE, response element (shows the locations of known p53 binding sites on the p21 promoter).

gene (Fig. 8C). Association of the H3K4me3 mark with this area of genes is well established (46). As no ChIP-seq data for H3K4me3 in RKO are available, we utilized the data from K562 cells and human umbilical vein endothelial cells (HUVEC), which we obtained from the ENCODE project (11). We saw a clear correlation between the H3K4me3 and HBO1 peaks surrounding the TSS of p21/CDKN1A, despite the fact that the two signals come from different cell lines and experimental conditions (Fig. 8C). Altogether, these data establish a strong global colocalization of the HBO1 complex with methylated H3K4 within the 5′ regions of genes, in a manner that is proportional to transcription levels. They also confirm that HBO1-JADE-dependent stimulation of the p21 gene occurs through ING-dependent association with H3K4me near the TSS.

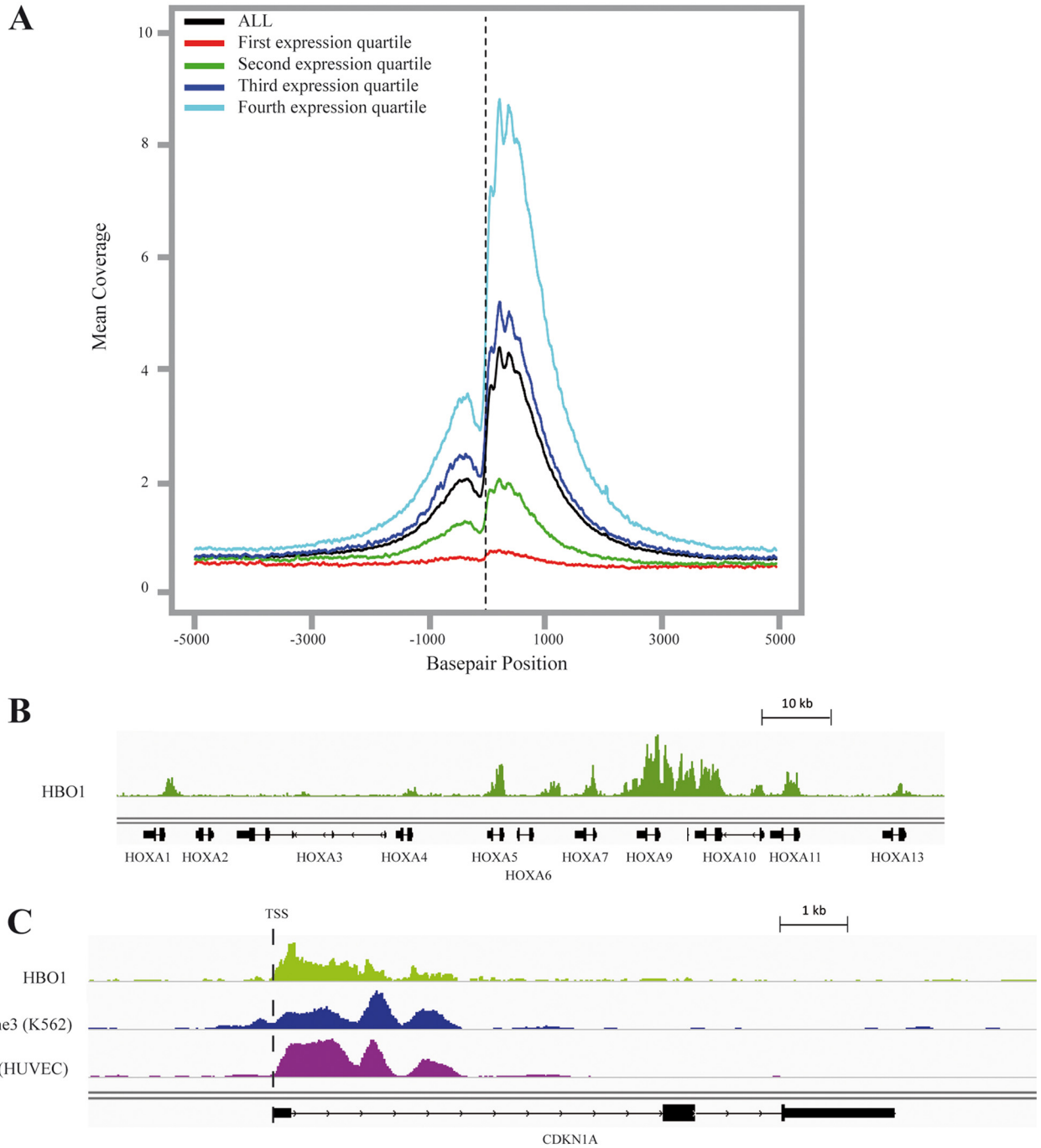

FIG 8 HBO1 is mainly located in the 5′ end of transcribed genes and colocalizes with H3K4me3. (A) HBO1 ChIP-seq signal intensity around the transcription start site (TSS) of genes in human RKO cells correlates globally with gene expression levels. The global profiles were produced using the UCSC genome browser gene definition and the Python package HTseq (see Materials and Methods). The binning of genes by their function or expression levels in RKO cells (70) was performed by subdividing genes in four equal categories (the fourth quartile includes the most highly expressed genes). (B) Enrichment of HBO1 signal over the HOXA cluster in the RKO cell line. (C) HBO1 signal is enriched in the 5′ region of the p21 coding region and colocalizes with the H3K4me3 signal. Our ChIP-seq HBO1 data from RKO cells aligned with the H3K4me3 signal from HUVEC and K562 cells obtained from the Broad Institute/ENCODE project (11).

DISCUSSION

MYST-ING HAT complexes are highly conserved in eukaryotes and play critical roles in genome expression and maintenance (2). In this study, we uncovered the conserved structural determinants for assembly of these complexes and their interaction with chromatin. By focusing our efforts on the human HBO1 complex, a major source of histone H4 and H3 acetylation *in vivo* (8, 23), we identified two short regions conserved in a subunit present in all MYST-ING complexes that are responsible for physical association of the MYST HAT enzyme and the ING tumor suppressor. In

a separate study on the MOZ/MORF complexes, deletions affecting these short conserved domains in the BRPF1 subunit also disrupted complex assembly (65). Importantly, our work identified a physiological regulation of the MYST-ING complex assembly that involves the natural occurrence of isoforms of the JADE1 protein produced by splice variants. One of these isoforms lacks the conserved region responsible for ING protein association (Fig. 2 and 3). This regulated association of ING proteins with HBO1 complexes was confirmed *in vivo* and was shown to have strong implications for the HBO1 HAT function (Fig. 4). Indeed, ING4/5 proteins contain a PHD finger domain that stimulates HBO1 HAT activity toward chromatin containing histone H3 trimethylated at lysine 4 (53), a mark found near the transcription start sites of active genes (57). This may well account for the reported roles of HBO1 in transcription regulation (2). It remains to be determined whether these interactions are important for the reported role of HBO1 in the initiation of DNA replication (35, 36). However, our previous work clearly indicated that the ING5 protein was critical for DNA synthesis *in vivo* (8).

A hallmark of MYST-ING complexes is the presence of multiple PHD finger domains within a single complex (Fig. 1B). We have previously analyzed the functions of the additional PHD modules present within the HBO1-associated JADE1 protein and found that they also bound histone H3 tails with high affinity, but with distinct specificity toward the K4 methylation status (53). While binding of the first PHD is completely inhibited by K4 methylation, the second PHD is largely unaffected. While we previously demonstrated the critical role of JADE1 PHD2 in chromatin binding and function of HBO1 complexes (53), our data also suggested the dominance of PHD1 within the double PHD/PZP structure in avoiding H3K4 methylation. We now show using NMR analysis that PHD1 alone produces the same chemical shift as the entire PZP domain when binding the histone H3 tail, supporting a single functional entity for interaction with chromatin (Fig. 5). These results have strong functional implications in light of the regulated association of ING4/5 with HBO1 complexes, which may occur not only through the use of JADE1 isoforms but also through external modulation. Intriguingly, multiple post-translational modifications, including S/T/Y phosphorylation and lysine acetylation have been mapped within conserved domain II of the scaffold subunits and within ING proteins in large-scale proteomic studies (7, 19, 47) (Fig. 3; see http://www.phosphosite.org or http://phosida.org). Thus, it is plausible that modification of the JADE-HBO1 complexes in response to various cellular events can alter their subunit composition, thereby regulating or retargeting their activity.

The molecular interactions that we described for MYST-ING complexes in general and HBO1-JADE-ING complexes in particular are critical for the function of these complexes, not only in binding and modification of specific regions of chromatin but also in their growth suppression activity linked to the ING tumor suppressors. We showed that only the isoform of JADE1 capable of interacting with ING proteins is able to slow growth and impair colony formation in soft agar, a signature of tumor suppressor activity (Fig. 6). In light of this, it is interesting to note that analysis of splice variants of JADE1 has shown that the ratio of the short to the long isoform greatly varies from 2 to 0.15 in a collection of over 300 cancer cell lines (15). This wide range of relative transcript levels suggests that regulation of JADE1 splicing can be used by some tumorigenic cell lines to impair the tumor suppressing function of the protein. This activity of JADE1L isoform implicates an induced senescence-like phenotype linked to upregulation of several interleukins and of the p21/CDKN1A gene and DNA damage checkpoint activation. These abilities of the JADE1 complex appear to be dependent on the associated HBO1 acetyltransferase, since siRNA-mediated depletion of this HAT leads to strong downregulation of the p21 gene. In fact, microarray analyses of gene expression indicate that loss of HBO1 leads to downregulation of a large number of genes linked to the p53 pathway of cell cycle control, senescence, and apoptosis. ING proteins have been implicated in these processes (61), and we now show evidence that they function through their association with MYST acetyltransferase complexes. In agreement with this model, a recent report has shown a functional interaction between MOZ and p53 in inducing p21 expression and cell cycle arrest (50). Our data now indicate that HBO1-JADE-ING complexes directly stimulate p53-dependent transcription of genes like p21 and that they are enriched near the transcription start site, where high levels of H3K4me3-containing chromatin exist, allowing them to associate with chromatin through the PHD finger domain of the ING tumor suppressors (Fig. 7 and 8). It is noteworthy to point out that the gene encoding LSD1/KDM1A, a major H3K4 demethylase and transcriptional repressor (26), is regulated in an opposite fashion upon increased JADE1L expression or HBO1 depletion (Fig. 6G), suggesting a function of the HBO1-JADE-ING complex in blocking H3K4 demethylation.

Our microarray experiments upon the manipulation of HBO1 and JADE1L protein levels also identified putative targeted genes and pathways that support important roles of this acetyltransferase complex in many cellular processes. In addition to the full set of p53 targets for cell cycle arrest and apoptosis, genes implicated in transcription repression, like components of deacetylase and demethylase complexes and factors involved in the maintenance of genomic DNA methylation (DNMT1-UHRF1), were upregulated during HBO1 depletion (Table 2). This suggests a significant increase in heterochromatinization of the genome in the treated cells and supports a global role of HBO1 in marking and stabilizing euchromatin, as evidenced by its global effect on H3/H4 acetylation (8, 23, 37). This is certainly in agreement with our ChIP-seq data that physically links HBO1 to the 5′ end of genes in a direct correlation to the level of transcription (Fig. 8). This bias toward the 5′ of genes was also recently obtained through ChIP-chip analysis in leukemic cells (37). Furthermore, while it has been argued that JADE1 is a direct repressor of Wnt signaling (6), we show here that HBO1 depletion leads to downregulation of repressors of the Wnt signaling pathway and upregulation of the frizzled receptors and BCL9, supporting a transcriptional role in modulating this pathway. Finally, it is interesting to note a likely compensation mechanism upon HBO1 depletion, as the gene for BRPF1 is upregulated, suggesting that MOZ/MORF complexes may compensate for the global loss of H3K14 acetylation (23). Mouse knockouts for HBO1 are embryonic lethal and show an almost complete loss of acetylated lysine 14 residue of histone H3 (H3K14ac) but an increase of H4K16ac (23). The latter phenotype could be explained by the downregulation of the Nuprin1/p8 inhibitor of the human MOF (hMOF) acetyltransferase, the MYST enzyme responsible for the bulk of H4K16ac (13, 59).

The work presented here highlights the highly conserved nature of the molecular interactions within the MYST-ING family of acetyltransferase complexes. It also demonstrates that the ING

tumor suppressor proteins function through their association with these complexes and chromatin regions carrying the H3K4me histone mark. It will be interesting to determine how this MYST-ING interaction is modulated to regulate cell proliferation. The multiple roles of these acetyltransferase complexes in genome expression and stability make them ideal targets and effectors for signaling events that regulate cell cycle progression.

ACKNOWLEDGMENTS

We are grateful to Or Gozani for the biotinylated histone peptides, Song Tan for recombinant HBO1, JADE1, and ING4 vectors and help in the early stages of this study, Mitch Smith for recombinant HBO1 vectors, and Maria Panchenko for JADE1S vectors.

This work was supported by grants from the Canadian Institutes of Health Research (CIHR) to J.C. (MOP-64289), the Canadian Cancer Society Research Institute to X.-J.Y., and the National Institutes of Health to T.G.K. N.A. held a CIHR/Institute of Aging fellowship, M.-E.L. held a National Science and Engineering Research Council Ph.D. studentship, K.C.G. holds an American Heart Association award, and Y.D. held a CIHR/Canada Graduate Scholarship. J.C. is a Canada Research Chair.

REFERENCES

1. **Acosta JC, et al.** 2008. Chemokine signaling via the CXCR2 receptor reinforces senescence. Cell **133**:1006–1018.
2. **Avvakumov N, Cote J.** 2007. The MYST family of histone acetyltransferases and their intimate links to cancer. Oncogene **26**:5395–5407.
3. **Bonner WM, et al.** 2008. GammaH2AX and cancer. Nat. Rev. Cancer **8**:957–967.
4. **Boudreault AA, et al.** 2003. Yeast enhancer of polycomb defines global Esa1-dependent acetylation of chromatin. Genes Dev. **17**:1415–1428.
5. **Champagne KS, et al.** 2008. The crystal structure of the ING5 PHD finger in complex with an H3K4me3 histone peptide. Proteins **72**:1371–1376.
6. **Chitalia VC, et al.** 2008. Jade-1 inhibits Wnt signalling by ubiquitylating beta-catenin and mediates Wnt pathway inhibition by pVHL. Nat. Cell Biol. **10**:1208–1216.
7. **Choudhary C, et al.** 2009. Lysine acetylation targets protein complexes and co-regulates major cellular functions. Science **325**:834–840.
8. **Doyon Y, et al.** 2006. ING tumor suppressor proteins are critical regulators of chromatin acetylation required for genome expression and perpetuation. Mol. Cell **21**:51–64.
9. **Doyon Y, Selleck W, Lane WS, Tan S, Cote J.** 2004. Structural and functional conservation of the NuA4 histone acetyltransferase complex from yeast to humans. Mol. Cell. Biol. **24**:1884–1896.
10. **el-Deiry WS, et al.** 1993. WAF1, a potential mediator of p53 tumor suppression. Cell **75**:817–825.
11. **Ernst J, et al.** 2011. Mapping and analysis of chromatin state dynamics in nine human cell types. Nature **473**:43–49.
12. **Foy RL, et al.** 2008. Role of Jade-1 in the histone acetyltransferase (HAT) HBO1 complex. J. Biol. Chem. **283**:28817–28826.
13. **Gironella M, et al.** 2009. p8/nupr1 regulates DNA-repair activity after double-strand gamma irradiation-induced DNA damage. J. Cell. Physiol. **221**:594–602.
14. **Gorrini C, et al.** 2007. Tip60 is a haplo-insufficient tumour suppressor required for an oncogene-induced DNA damage response. Nature **448**: 1063–1067.
15. **Greshock J, et al.** 2010. Molecular target class is predictive of in vitro response profile. Cancer Res. **70**:3677–3686.
16. **Groppo R, Richter JD.** 2011. CPEB control of NF-kappaB nuclear localization and interleukin-6 production mediates cellular senescence. Mol. Cell. Biol. **31**:2707–2714.
17. **Howe L, et al.** 2002. Yng1p modulates the activity of Sas3p as a component of the yeast NuA3 histone acetyltransferase complex. Mol. Cell. Biol. **22**:5047–5053.
18. **Hung T, et al.** 2009. ING4 mediates crosstalk between histone H3 K4 trimethylation and H3 acetylation to attenuate cellular transformation. Mol. Cell **33**:248–256.
19. **Huttlin EL, et al.** 2010. A tissue-specific atlas of mouse protein phosphorylation and expression. Cell **143**:1174–1189.
20. **Jia D, Jurkowska RZ, Zhang X, Jeltsch A, Cheng X.** 2007. Structure of Dnmt3a bound to Dnmt3L suggests a model for de novo DNA methylation. Nature **449**:248–251.
21. **Jung YS, Qian Y, Chen X.** 2010. Examination of the expanding pathways for the regulation of p21 expression and activity. Cell Signal. **22**:1003–1012.
22. **Kouzarides T.** 2007. Chromatin modifications and their function. Cell **128**:693–705.
23. **Kueh AJ, Dixon MP, Voss AK, Thomas T.** 2011. HBO1 is required for H3K14 acetylation and normal transcriptional activity during embryonic development. Mol. Cell. Biol. **31**:845–860.
24. **Kuilman T, et al.** 2008. Oncogene-induced senescence relayed by an interleukin-dependent inflammatory network. Cell **133**:1019–1031.
25. **Lan F, et al.** 2007. Recognition of unmethylated histone H3 lysine 4 links BHC80 to LSD1-mediated gene repression. Nature **448**:718–722.
26. **Lan F, Nottke AC, Shi Y.** 2008. Mechanisms involved in the regulation of histone lysine demethylases. Curr. Opin. Cell Biol. **20**:316–325.
27. **Latham JA, Dent SY.** 2007. Cross-regulation of histone modifications. Nat. Struct. Mol. Biol. **14**:1017–1024.
28. **Li B, et al.** 2007. Combined action of PHD and chromo domains directs the Rpd3S HDAC to transcribed chromatin. Science **316**:1050–1054.
29. **Li H, Durbin R.** 2009. Fast and accurate short read alignment with Burrows-Wheeler transform. Bioinformatics **25**:1754–1760.
30. **Li H, et al.** 2006. Molecular basis for site-specific read-out of histone H3K4me3 by the BPTF PHD finger of NURF. Nature **442**:91–95.
31. **Lin SM, Du P, Huber W, Kibbe WA.** 2008. Model-based variance-stabilizing transformation for Illumina microarray data. Nucleic Acids Res. **36**:e11.
32. **Liu Y, Subrahmanyam R, Chakraborty T, Sen R, Desiderio S.** 2007. A plant homeodomain in RAG-2 that binds hypermethylated lysine 4 of histone H3 is necessary for efficient antigen-receptor-gene rearrangement. Immunity **27**:561–571.
33. **Martin DG, et al.** 2006. The Yng1p plant homeodomain finger is a methyl-histone binding module that recognizes lysine 4-methylated histone H3. Mol. Cell. Biol. **26**:7871–7879.
34. **Matthews AG, et al.** 2007. RAG2 PHD finger couples histone H3 lysine 4 trimethylation with V(D)J recombination. Nature **450**:1106–1110.
35. **Miotto B, Struhl K.** 2010. HBO1 histone acetylase activity is essential for DNA replication licensing and inhibited by geminin. Mol. Cell **37**:57–66.
36. **Miotto B, Struhl K.** 2008. HBO1 histone acetylase is a coactivator of the replication licensing factor Cdt1. Genes Dev. **22**:2633–2638.
37. **Mishima Y, et al.** 2011. The Hbo1-Brd1/Brpf2 complex is responsible for global acetylation of H3K14 and required for fetal liver erythropoiesis. Blood **118**:2443–2453.
38. **Nagashima M, et al.** 2001. DNA damage-inducible gene p33ING2 negatively regulates cell proliferation through acetylation of p53. Proc. Natl. Acad. Sci. U. S. A. **98**:9671–9676.
39. **Nagashima M, et al.** 2003. A novel PHD-finger motif protein, p47ING3, modulates p53-mediated transcription, cell cycle control, and apoptosis. Oncogene **22**:343–350.
40. **Panchenko MV, Zhou MI, Cohen HT.** 2004. von Hippel-Lindau partner Jade-1 is a transcriptional co-activator associated with histone acetyltransferase activity. J. Biol. Chem. **279**:56032–56041.
41. **Pena PV, et al.** 2006. Molecular mechanism of histone H3K4me3 recognition by plant homeodomain of ING2. Nature **442**:100–103.
42. **Perry J.** 2006. The Epc-N domain: a predicted protein-protein interaction domain found in select chromatin associated proteins. BMC Genomics **7**:6.
43. **Piche B, Li G.** 2010. Inhibitor of growth tumor suppressors in cancer progression. Cell. Mol. Life Sci. **67**:1987–1999.
44. **Qin S, et al.** 2011. Recognition of unmodified histone H3 by the first PHD finger of bromodomain-PHD finger protein 2 provides insights into the regulation of histone acetyltransferases MOZ and MORF. J. Biol. Chem. **286**:36944–36955.
45. **Ramon-Maiques S, et al.** 2007. The plant homeodomain finger of RAG2 recognizes histone H3 methylated at both lysine-4 and arginine-2. Proc. Natl. Acad. Sci. U. S. A. **104**:18993–18998.
46. **Rando OJ, Chang HY.** 2009. Genome-wide views of chromatin structure. Annu. Rev. Biochem. **78**:245–271.
47. **Rikova K, et al.** 2007. Global survey of phosphotyrosine signaling identifies oncogenic kinases in lung cancer. Cell **131**:1190–1203.
48. **Rodier F, Campisi J.** 2011. Four faces of cellular senescence. J. Cell Biol. **192**:547–556.
49. **Rodier F, et al.** 2009. Persistent DNA damage signalling triggers

senescence-associated inflammatory cytokine secretion. Nat. Cell Biol. **11**: 973–979.
50. **Rokudai S, et al.** 2009. Monocytic leukemia zinc finger (MOZ) interacts with p53 to induce p21 expression and cell-cycle arrest. J. Biol. Chem. **284**:237–244.
51. **Russell M, Berardi P, Gong W, Riabowol K.** 2006. Grow-ING, Age-ING and Die-ING: ING proteins link cancer, senescence and apoptosis. Exp. Cell Res. **312**:951–961.
52. **Ruthenburg AJ, Allis CD, Wysocka J.** 2007. Methylation of lysine 4 on histone H3: intricacy of writing and reading a single epigenetic mark. Mol. Cell **25**:15–30.
53. **Saksouk N, et al.** 2009. HBO1 HAT complexes target chromatin throughout gene coding regions via multiple PHD finger interactions with histone H3 tail. Mol. Cell **33**:257–265.
54. **Saksouk N, Avvakumov N, Cote J.** 2008. (de)MYSTification and INGenuity of tumor suppressors. Cell. Mol. Life Sci. **65**:1013–1018.
55. **Selleck W, Fortin I, Sermwittayawong D, Cote J, Tan S.** 2005. The Saccharomyces cerevisiae Piccolo NuA4 histone acetyltransferase complex requires the Enhancer of Polycomb A domain and chromodomain to acetylate nucleosomes. Mol. Cell. Biol. **25**:5535–5542.
56. **Shi X, et al.** 2006. ING2 PHD domain links histone H3 lysine 4 methylation to active gene repression. Nature **442**:96–99.
57. **Shilatifard A.** 2006. Chromatin modifications by methylation and ubiquitination: implications in the regulation of gene expression. Annu. Rev. Biochem. **75**:243–269.
58. **Shiseki M, et al.** 2003. p29ING4 and p28ING5 bind to p53 and p300, and enhance p53 activity. Cancer Res. **63**:2373–2378.
59. **Smith ER, et al.** 2005. A human protein complex homologous to the Drosophila MSL complex is responsible for the majority of histone H4 acetylation at lysine 16. Mol. Cell. Biol. **25**:9175–9188.
60. **Smyth GK.** 2004. Linear models and empirical Bayes methods for assessing differential expression in microarray experiments. Stat. Appl. Genet. Mol. Biol. **3**:Article3.
61. **Soliman MA, Riabowol K.** 2007. After a decade of study-ING, a PHD for a versatile family of proteins. Trends Biochem. Sci. **32**:509–519.
62. **Stankunas K, et al.** 1998. The enhancer of polycomb gene of Drosophila encodes a chromatin protein conserved in yeast and mammals. Development **125**:4055–4066.
63. **Taverna SD, et al.** 2006. Yng1 PHD finger binding to H3 trimethylated at K4 promotes NuA3 HAT activity at K14 of H3 and transcription at a subset of targeted ORFs. Mol. Cell **24**:785–796.
64. **Taverna SD, Li H, Ruthenburg AJ, Allis CD, Patel DJ.** 2007. How chromatin-binding modules interpret histone modifications: lessons from professional pocket pickers. Nat. Struct. Mol. Biol. **14**:1025–1040.
65. **Ullah M, et al.** 2008. Molecular architecture of quartet MOZ/MORF histone acetyltransferase complexes. Mol. Cell. Biol. **28**:6828–6843.
66. **Utley RT, Lacoste N, Jobin-Robitaille O, Allard S, Cote J.** 2005. Regulation of NuA4 histone acetyltransferase activity in transcription and DNA repair by phosphorylation of histone H4. Mol. Cell. Biol. **25**:8179–8190.
67. **Vermeulen M, et al.** 2007. Selective anchoring of TFIID to nucleosomes by trimethylation of histone H3 lysine 4. Cell **131**:58–69.
68. **Voss AK, Collin C, Dixon MP, Thomas T.** 2009. Moz and retinoic acid coordinately regulate H3K9 acetylation, Hox gene expression, and segment identity. Dev. Cell **17**:674–686.
69. **Voss AK, Thomas T.** 2009. MYST family histone acetyltransferases take center stage in stem cells and development. Bioessays **31**:1050–1061.
70. **West JD, Marnett LJ.** 2005. Alterations in gene expression induced by the lipid peroxidation product, 4-hydroxy-2-nonenal. Chem. Res. Toxicol. **18**:1642–1653.
71. **Wysocka J, et al.** 2006. A PHD finger of NURF couples histone H3 lysine 4 trimethylation with chromatin remodelling. Nature **442**:86–90.
72. **Yang XJ, Ullah M.** 2007. MOZ and MORF, two large MYSTic HATs in normal and cancer stem cells. Oncogene **26**:5408–5419.
73. **Ythier D, Larrieu D, Brambilla C, Brambilla E, Pedeux R.** 2008. The new tumor suppressor genes ING: genomic structure and status in cancer. Int. J. Cancer **123**:1483–1490.
74. **Zhou MI, et al.** 2005. Jade-1, a candidate renal tumor suppressor that promotes apoptosis. Proc. Natl. Acad. Sci. U. S. A. **102**:11035–11040.
75. **Zhou MI, Wang H, Foy RL, Ross JJ, Cohen HT.** 2004. Tumor suppressor von Hippel-Lindau (VHL) stabilization of Jade-1 protein occurs through plant homeodomains and is VHL mutation dependent. Cancer Res. **64**:1278–1286.
76. **Zhou MI, et al.** 2002. The von Hippel-Lindau tumor suppressor stabilizes novel plant homeodomain protein Jade-1. J. Biol. Chem. **277**:39887–39898.